ChemPubSoc Europe

DOI: 10.1002/cphc.201600653

CHEMPHYSCHEM Articles

Entropy Drives Calcium Carbonate Ion Association

Matthias Kellermeier[+],[a] Paolo Raiteri[+],[b] John K. Berg,[c] Andreas Kempter,[d] Julian D. Gale,[b] and Denis Gebauer*[c]

The understanding of the molecular mechanisms underlying the early stages of crystallisation is still incomplete. In the case of calcium carbonate, experimental and computational evidence suggests that phase separation relies on so-called pre-nucleation clusters (PNCs). A thorough thermodynamic analysis of the enthalpic and entropic contributions to the overall free energy of PNC formation derived from three independent methods demonstrates that solute clustering is driven by entropy. This can be quantitatively rationalised by the release of water molecules from ion hydration layers, explaining why ion association is not limited to simple ion pairing. The key role of water release in this process suggests that PNC formation should be a common phenomenon in aqueous solutions.

1. Introduction

Nucleation of solid particles from supersaturated solutions is an elementary step in any reaction that involves crystallisation or precipitation, and thus is of inherent importance to numerous processes and applications.[1,2] However, despite extensive research in this field for more than a century,[3,4] the actual mechanisms of the onset and progress of phase separation are still under considerable debate, as reflected in a rapidly increasing number of related studies over the past few years.[5–12] This has led to the development of so-called "non-classical" nucleation models, such as the pre-nucleation cluster (PNC) pathway,[6,10] or two-step nucleation for protein crystallisation.[13–15]

In the case of calcium carbonate, which is the most abundant biomineral[16] and a compound of great industrial, economic and ecological relevance,[17] it has been demonstrated that precipitation from solution can involve a complex sequence of processes, which may include ion clustering and often results in nanoparticles of amorphous calcium carbonate (ACC) as the initial solid phase.[10,18] One particularly contentious point concerns the question as to why solute association is not limited to ion paring, but rather proceeds to yield larger entities (PNCs) of a chain-like structural form called DOLLOP (dynamically ordered liquid-like oxyanion polymer).[19] Elucidating the thermodynamic driving force for PNC formation can provide mechanistic clues to contribute to this debate. Therefore, we have explored calcium carbonate clustering in dilute solutions by temperature-dependent potentiometric titrations and isothermal titration calorimetry (ITC), complemented by molecular dynamics (MD) simulations. Our results demonstrate that ion association is favoured owing to an increase in entropy, while the enthalpic balance of the process is endothermic. This demonstrates the importance of the assessment of the balance between entropy and enthalpy for solute association beyond colloidal systems,[20,21] while a molecular explanation for the entropic driving force underlying ion association provides a mechanistic clue why it is not limited to ion pairing.

2. Results and Discussion

In order to study ion association in dilute $CaCO_3$ solutions at different temperatures, we applied a titration technique that was previously used for the quantification of PNC formation under ambient conditions.[22–24] For all investigated temperatures (10–60 °C), considerable fractions of Ca^{2+} ions are bound in ion associates in the pre-nucleation regime (Figure S1 in the Supporting Information). An increasing amount of calcium is bound at constant pH as the temperature increases (Figure S2). The binding of carbonate ions during titration can be independently assessed by using the volumes of NaOH added to maintain the pH of the solutions at a constant level,[23] showing that equal amounts of Ca^{2+} and CO_3^{2-} ions are bound during all stages of the experiments at all of the temperatures studied (Figure S3). This is further corroborated by simultaneous conductivity measurements, underlining that association of Ca^{2+} and HCO_3^- does not occur to any significant extent at the given conditions (Figure S4).[22] The free ion products [IP, $c_{free}(Ca^{2+})\cdot c_{free}(CO_3^{2-})$] were calculated,[23] and show a linear increase when plotted versus the amount of Ca^{2+} added until

[a] Dr. M. Kellermeier[+]
Material Physics, BASF SE
D-67056 Ludwigshafen (Germany)

[b] Prof. Dr. P. Raiteri,[+] Prof. Dr. J. D. Gale
Department of Chemistry, Curtin Institute for Computation and Institute for Geoscience Research
Curtin University
PO Box U1987, Perth, WA 6845 (Australia)

[c] Dr. J. K. Berg, Dr. D. Gebauer
Department of Chemistry, Physical Chemistry
University of Konstanz
Universitätsstraße 10, D-78464 Konstanz (Germany)
E-mail: Denis.Gebauer@uni-konstanz.de

[d] Dr. A. Kempter
Reactive Systems and Inorganic Nanomaterials Research, BASF SE
D-67056 Ludwigshafen (Germany)

[+] These authors contributed equally

Supporting Information for this article can be found under: http://dx.doi.org/10.1002/cphc.201600653.

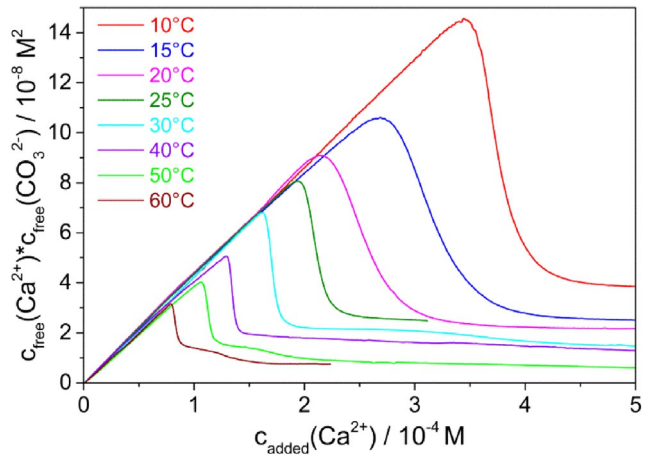

Figure 1. Profiles of the measured free ion products upon addition of Ca^{2+} into carbonate buffers at pH 9.50 and different temperatures (as indicated).

a maximum is reached, where nucleation becomes evident (Figure 1). Subsequently, the free ion products drop to levels that represent the solubility of the precipitated polymorph, which is usually ACC in these experiments.[22] With increasing temperature, the critical IP required for nucleation to occur decreases, as does the solubility of the initially formed solid phase (Figure S5).

The stability of ion associates in solution (i.e. their formation constant) is directly reflected in the slopes of the IP plots prior to nucleation, with lines exhibiting a smaller gradient being indicative of stronger binding, and hence more stable ion associates. The data in Figure 1 suggest that thermodynamic stability increases with temperature, as is evident from the slight flattening observed at 40–60 °C.

The binding data obtained by potentiometric titration can be evaluated quantitatively by utilizing different speciation models. The simplest model, ion pairing between Ca^{2+} and CO_3^{2-}, would lead to linear binding profiles,[23] consistent with what is observed experimentally in the pre-nucleation stage. On the other hand, the so-called multiple-binding equilibrium[22] approach accounts for the formation of species larger than simple ion pairs (i.e. PNCs). The fundamental assumption underlying this model is that all binding events between calcium and carbonate ions are equal and independent, that is, binding a calcium ion to an ion pair, or an ion pair to an ion pair, etc., is energetically the same as binding a calcium ion to a single carbonate ion. Formally, in the law of mass action, all associated states are then indiscernible as per the assumption made, and cluster formation can only be treated quantitatively when bound $CaCO_3$ is specified as a generic "cluster" rather than a simple "ion pair".[24] Under these circumstances, the multiple-binding model also predicts linear binding profiles.[19,23,24] Thus, as an immediate consequence it follows that binding data alone do not allow one to distinguish between simple ion pairing and cluster formation, or in other words, linear binding profiles do not unequivocally rule out the presence of a significant population of higher associated states (as put forward in previous work).[10,19,22–24] At this point, additional experiments are required to prove that larger clusters do exist, as demonstrated in previous work employing analytical ultracentrifugation,[22,23] which shows that the bound $CaCO_3$—pre-nucleation—quantitatively resides in entities significantly larger than ion pairs,[24] cryogenic transmission electron microscopy (Cryo TEM)[25,26] and scattering techniques.[26] Moreover, the computer simulations described by Demichelis et al.[19] provide further evidence for the occurrence of larger clusters in equilibrium and explicitly support the basic assumption of equal and independent binding events: in the simulations, all populations of associated states were a priori fitted with individual equilibrium constants, but it turned out that they were in fact all equal to within the statistical uncertainty.

Experimental association constants [K_{IP}(Cluster)] obtained on the basis of the multiple-binding equilibrium generally represent the formation of $CaCO_3$ ion pairs within pre-nucleation clusters, relative to the state of free (non-bound) ions and averaged over all cluster sizes (thus also including the ion pair).[24] Using this model, we have derived K_{IP}(Cluster) and the corresponding Gibbs free energy of reaction [ΔG_{IP}(Cluster) $= -RT \ln K_{IP}$] from the titration data at each studied temperature (see SI Section 1.1). The resulting temperature dependence of ΔG_{IP}(Cluster) is shown in Figure 2 (red circles), individual values of K_{IP}(Cluster) and ΔG_{IP}(Cluster) are compiled in Table S1.

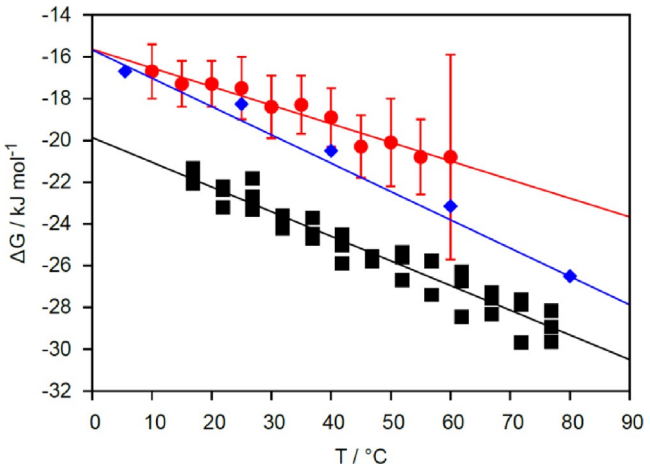

Figure 2. Plot of the Gibbs free energy for the formation of $CaCO_3$ ion pairs within pre-nucleation clusters, ΔG_{IP}(Cluster), as a function of temperature at standard pressure and concentration (1 M), determined by potentiometric titrations (red circles). For comparison, ΔG values reported for the formation of "$CaCO_3^{0}$" ion pairs in previous work[27] are also included (blue diamonds), as are the results obtained from MD simulations (black squares) for an isolated ion pair. Note that triplicate simulations were performed from different initial configurations at each temperature, and all data points are shown to indicate the level of statistical uncertainty. See section 2.2 in the Supporting Information for discussion of the relationship between binding free energies in pre-nucleation clusters and for the ion pair alone.

An alternative way to study the interaction of calcium and carbonate ions in solution at the atomic level are MD simulations. Provided the underlying potential-energy surface is accurate, the equilibrium constant for pure ion pairing alone can be determined theoretically. The force-field model used for the aqueous calcium carbonate system in the present work has been carefully validated against numerous pieces of experimental thermodynamic data, including the relative phase sta-

bility of calcite, aragonite and vaterite, the free energy of hydration of dissolved Ca^{2+} and CO_3^{2-} ions, and the solubility product of calcite.[28] Therefore, this model should be capable of describing the competition between water and other ions in the coordination shell of the various species that occur in this environment. On this basis, we have performed metadynamics simulations of a single calcium and a single carbonate ion in water to determine the free-energy profile as a function of the Ca–C distance over a similar temperature range as in the experimental titration measurements discussed above. The results are shown in Figure 3. Three distinct states can be identified in the profile. At just greater than 7 Å, there is a broad minimum corresponding to the (doubly) solvent-separated state, where the two first solvation shells of the ions come into contact. Just below a Ca–C distance of 5 Å, we observe a second minimum in the free energy owing to the solvent-shared ion pair. Finally, below 4 Å, there is a split minimum attributable to the contact ion pair. The inner and outer states within this minimum correspond to the bidentate and monodentate coordination of carbonate to calcium, respectively. As the temperature increases, the presence of the bidentate state becomes more evident, though the monodentate state remains thermodynamically favoured.

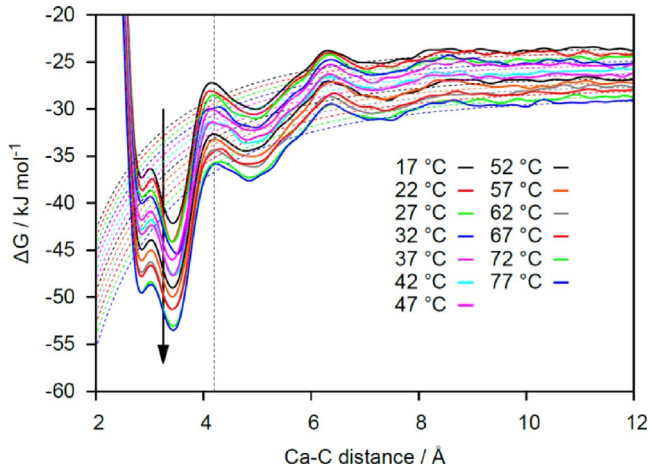

Figure 3. Free-energy profile for the interaction between a single calcium and a single carbonate ion in water as a function of the Ca–C distance for one of the repeats. Curves are shown for temperatures of 17 to 77 °C in intervals of 5 K. Curves are displaced vertically for ease of visualisation, while noting that the absolute free energy at any given distance is only defined to within an additive constant.

The key question now is how to determine the free energy of ion pairing from these data. Although the ΔG curves initially appear to reach a plateau beyond 9 Å, this is deceptive. Ultimately, the configurational entropy (which varies as the logarithm of the square of the Ca–C distance because of the volume available) will result in the free energy decreasing again at large distances. Here we have taken the upper bound to ion association to be the Bjerrum radius, as given by Fuoss and Kraus,[29] which conceptually corresponds to the point where the electrostatic interaction between the ions is of the same order of magnitude as ambient thermal energy. However, given that the free-energy curves shown in Figure 3 are relatively flat in this region, the results are only slightly sensitive to the choice of the boundary chosen for the associated state. Included in the calculation of the ion pairing free energies is the correction of the standard state to 1 M.

Values for the free energy of ion pairing obtained from the MD simulations are shown as black squares together with the data from the potentiometric titrations in Figure 2. When comparing the theoretical and experimental data, there is an important point to discuss. In the simulations performed here, the free energy is extracted as a function of temperature for a single ion pair in aqueous solution. However, in the case of the experiments, the free energies are determined from binding equilibria in which the ion pairs can also be part of a PNC. Therefore, the values are a weighted average of the free energy of isolated ion pairing and the corresponding values within the cluster environment, including all states of association and thus averaging over all possible association numbers. As such, the theoretical and experimental data might not be directly comparable. In previous work, the free energies of ion pairing and for association of ion pairs into PNCs were determined by fitting a speciation model to equilibrium simulation results.[19] It was found that the free energy of association between ion pairs within PNCs is only 1.4 kJ mol^{-1} (per ion pair) more exothermic than for ion pairing itself, and thus the binding strength of ion pairs is actually very similar regardless of whether they are isolated or part of a pre-nucleation cluster.

The free energy of ion pairing, both in isolation and within PNCs, decreases with increasing temperature. This trend, as well as the measured absolute values of ΔG, are in line with the results of an early study (blue diamonds in Figure 2),[27] where the formation of calcium carbonate ion pairs ("$CaCO_3^{0}$") was investigated at different temperatures. However, in this previous work, the temperature-dependent values of ΔG were not analysed with respect to enthalpic and entropic contributions, and the existence of larger clusters was not considered.

Another independent experimental technique to quantify enthalpic and entropic contributions to ion association in calcium carbonate solutions at a given temperature is isothermal titration calorimetry, where volume increments of dilute $CaCl_2$ solution are dosed into carbonate buffer and the heating rate required for maintaining a constant temperature after each addition step is measured. Typical raw data from such an experiment at 25 °C are plotted in Figure S6, whereas Figure 4 shows processed results, that is, the average heat per mole of injected Ca^{2+} ions as a function of the total calcium concentration in the system, corrected for the heat of dilution. First of all, it is worth noting that there are no statistically significant kinks (or steps) in the data, which would indicate a first-order phase transition.[30] This suggests that our measurements indeed reflect pre-nucleation, or more generically speaking, single-phase solution states—note that the levels of supersaturation reached at the end of the ITC experiments ($IP_{analytical} \approx 2.8 \times 10^{-7}$ M^2) were in the range of critical values determined by potentiometric titration at the same temperature ($IP_{analytical} \approx 2.5 \times 10^{-7}$ M^2 at the maximum, cf. Figure S4), and that no precipitation was observed in the calorimeter. In the present case, we assume that only solute ion association occurs within a single-

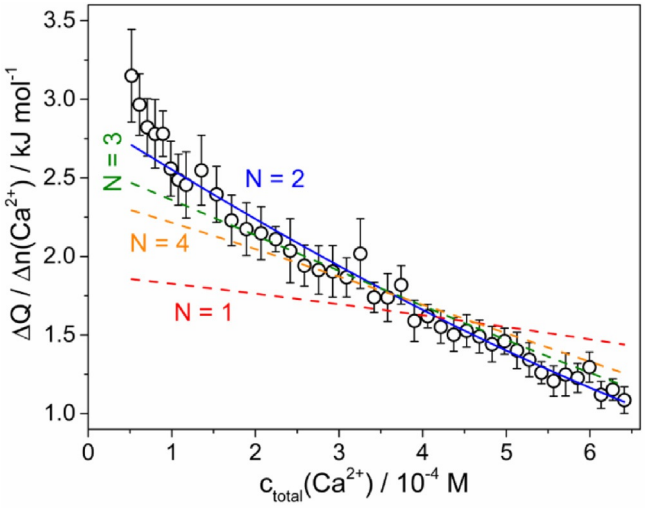

Figure 4. Isothermal titration calorimetry data obtained by repeated dosing of $CaCl_2$ into $NaHCO_3/Na_2CO_3$ buffer at pH 9.50 and 25 °C. Black circles represent the measured heat (ΔQ) per mole of injected Ca^{2+} ($\pm$1-σ-standard deviation based on 5 independent measurements) as a function of the total calcium concentration. Best fits based on a simple ion pairing approach and the multiple-binding model are shown as red dashed ($R^2 = 0.42221$) and blue lines ($R^2 = 0.97195$), respectively. Fits were performed using Equations 6 and 7 (SI), with the calcium–carbonate coordination number N set to 1 for ion pairing and 2 for PNC formation, as detailed in section 1.2 in the Supporting Information. In the latter case, K_{IP}(Cluster) was determined to be $1115 \pm 230\ M^{-1}$ [values for ΔH_{IP}(Cluster) and ΔS_{IP}(Cluster) are given in Table 1 in the main manuscript]. Fits for higher coordination numbers, as expected for droplets of a dense liquid phase (DLP), show progressively worse correlation with the experimental data (green dashed line: $N = 3$, $R^2 = 0.92496$; orange dashed line: $N = 4$, $R^2 = 0.83931$).

phase system, and evaluate the ITC data based on two distinct thermodynamic speciation models, that is, ion pairing and multiple-binding equilibrium (cf. section 1.1 in the Supporting Information), to obtain ΔH_{IP}(Cluster) and K_{IP}(Cluster) [and with it, ΔS_{IP}(Cluster)]. Corresponding fits are shown as dashed red (ion pairing, $N = 1$), full blue (multiple binding with a calcium–carbonate coordination number of $N = 2$), as well as dashed green and orange lines (multiple binding with $N = 3$ and $N = 4$, respectively) in Figure 4.

It is evident that the multiple-binding equilibrium model with $N = 2$, which is consistent with chain- or ring-like structures of alternating cations and anions according to the DOLLOP concept,[19] shows the best fit of the data. Increased coordination numbers of $N = 3$ or $N = 4$ (which qualitatively correspond to internal condensation within PNCs) lead to a reduction in the quality of the fit. Most significantly, simple ion pairing ($N = 1$) cannot describe the slope of the data. This does not change when activity coefficients are taken into account during data evaluation, because the ionic strength of the sample remains more or less constant ($\pm$10%) throughout the ITC experiment and hence consideration of activity coefficients will not affect the relative quality of the fits according to the different models. It should be noted, however, that the ion-pairing model could be extended by additional fitting parameters (e.g. including the formation of $Ca(CO_3)_2^{2-}$ due to the given excess of carbonate), and thereby be modified to fit the data.

Hence, at this point, while the ITC data provides evidence for ion association beyond the ion pair, it does not necessarily and unambiguously distinguish between PNCs in the form of DOLLOP and charged multiple ion complexes. Either way, it is evident that simple ion pairing has to be extended by at least one additional parameter, which may or may not relate directly to the occurrence of multiple binding (i.e. the x parameter in Equation 4 in section 1.1 in the Supporting Information). This is in line with the evidence that $CaCO_3$ ion association in solution is not limited to ion pairs, but indeed involves the formation of larger species, as shown unambiguously by additional analytical techniques in previous works.[22,26] In order to directly confirm the assumption of temperature-independent enthalpies and entropies experimentally, we have performed additional ITC measurements at another temperature (40 °C). Again, the resulting data can be well described by fits according to the multiple-binding equilibrium model with $N = 2$ (SI Figure S7). The enthalpy and entropy values obtained from these measurements are virtually identical to those determined at 25 °C (Table 1), thus verifying the presumed temperature independence of ΔH_{IP}(Cluster) and ΔS_{IP}(Cluster) in the studied temperature range.

Table 1. Enthalpic and entropic contributions to the free energy of PNC formation in the $CaCO_3$ system, as determined experimentally by potentiometric titration and ITC. Theoretical values for ion pairing computed using metadynamics[31] simulations are given for comparison.

	ΔH_{IP}(Cluster) [kJ mol^{-1}]	ΔS_{IP}(Cluster) [J K^{-1} mol^{-1}]
potentiometric titration	8.7 ± 2.4	89 ± 8
ITC (25 °C)	7.4 ± 2.8	83 ± 12
ITC (40 °C)	8.2 ± 2.4	86 ± 9
MD simulations[a]	12.4 ± 1.7	118 ± 5.4

[a] Note that simulations were performed for one ion pair at infinite dilution and then corrected to standard conditions; nevertheless, the data can be compared with the experimental results for PNC formation, see section 2.2 in the Supporting Information.

The ΔG(T) data from potentiometric titration and MD simulations can be used to evaluate changes in enthalpy and entropy during PNC formation, when assuming that both ΔH and ΔS are independent of temperature over the studied range. As $\Delta G = \Delta H - T\Delta S$, the enthalpy [$\Delta H_{IP}$(Cluster)] and entropy [$\Delta S_{IP}$(Cluster)] of ion association can then be determined from the extrapolation to $T = -273.15$ °C and slope of linear fits to the data in Figure 2 (full lines), respectively. Corresponding results are listed in Table 1, together with those from ITC discussed above. It can be seen that enthalpic and entropic contributions determined by ITC and potentiometric titration essentially agree to within statistical accuracy. This strongly supports the reliability of the data and the validity of the assumptions made, in particular with respect to constant enthalpies and entropies over the range of temperatures studied.

Considering the enthalpies reported in Table 1, it becomes immediately evident that pre-nucleation ion association is a slightly endothermic process. This means that Coulomb

forces, representing the strongest and longest-ranged type of interaction in aqueous ionic systems, do not significantly contribute to the thermodynamic stability of the clusters. Quite the contrary, the binding of ions in PNCs appears to be accompanied by minor costs in enthalpy. This energetic penalty can be understood as a decrease in the number of favourable ion–dipole interactions of Ca^{2+} and CO_3^{2-} ions with water molecules in their hydration layers, which is not compensated by the formation of ionic bonds. From this point of view, the minor costs in enthalpy linked to the formation of pre-nucleation clusters appear realistic and originate from slightly less favourable average interactions in all associated states relative to the free ions in solution.

It follows inevitably that pre-nucleation association of calcium and carbonate ions is a process that is predominantly driven by entropy (Table 1). The main entropic contribution lies in the relative number of water molecules bound in the hydration layers of free ions and associated states. The release of coordinated water upon "polycondensation" of Ca^{2+} and CO_3^{2-} into both ion pairs and subsequently DOLLOPs leads to an increase in entropy, which essentially arises from a gain in translational and rotational degrees of freedom of the water molecules. Such entropic terms have been invoked as a crucial factor in protein folding[32,33] and allosteric regulation,[34] are regarded as the major driving force for micellisation,[35] are important for biomolecular recognition[36] as well as metal complex formation with multidentate ligands[37] and also play a key role in the self-assembly of colloids into crystal structures.[38] In the present case, the fact that the entropic driving force is associated with the return of water to bulk solution is consistent with the observation that the temperature dependence of the free energy is very similar for both ion pairing in pre-nucleation clusters (as determined experimentally) and when isolated in aqueous solution (from simulation). We note that this loss of hydration water as an entropic factor has previously been found significant in the crystallisation of proteins, specifically for haemoglobin.[39] The present study provides experimental evidence demonstrating that this extends to the initial stages of mineral formation.

In aqueous solution, the first hydration layer of Ca^{2+} ions contains about 7 water molecules,[28,40–42] whereas CO_3^{2-} ions are coordinated by either 9 or 12 water molecules in the first shell, based on experiment and simulation, respectively.[43,44] When considering only the first hydration shell, our molecular dynamics simulations (Figure 5) suggest that the isolated ion pair is coordinated by 15 water molecules and hence, 4 water molecules are released upon binding. According to the estimates of Dunitz,[45] the upper bound for the entropy change associated with water going from a crystalline environment, where it is relatively immobile, to the liquid phase is 29.3 $JK^{-1}mol^{-1}$. The actual values for the hydrates of calcium carbonate, monohydrocalcite and ikaite, are slightly higher than this at 32 and 33.5 $JK^{-1}mol^{-1}$, respectively.[46,47] Based on this, both the measured and calculated entropy changes would equate to the loss of approximately 3 water molecules from the hydration shell, which is slightly lower than the observed value. Given the underlying assumption that the water bound to the ions is as immobile as that in a hydrate salt, which is not the case in reality, there is reasonable consistency between the thermodynamics and a physical interpretation in terms of the release of water from the solvation shells of the individual ions on binding.

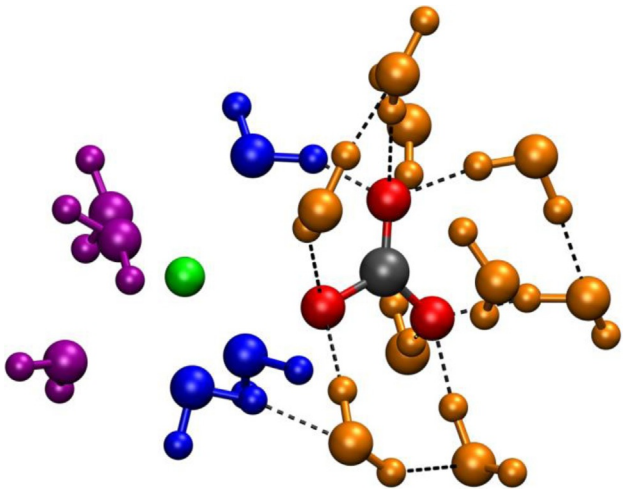

Figure 5. Snapshot of the hydration environment of the $CaCO_3$ ion pair taken from a molecular dynamics simulation. Here the calcium, carbon and oxygen atoms of the ion pair are coloured green, black and red, respectively. Water molecules are coloured according to the species to which they are coordinated: purple and orange represent water bound to Ca^{2+} and hydrogen-bonded (indicated by dashed black lines) to CO_3^{2-}, respectively, while blue-coloured water molecules are those that are bridging between calcium and carbonate. The total average number of water molecules in the first shell is 15, only the water molecules within 3.5 Å of the Ca and carbonate oxygen are shown. A snapshot with the typical water structure around a dissociated ion pair is shown in the SI (Figure S8).

3. Conclusions

In conclusion, our thermodynamic analyses show that entropy is the key to ion association in dilute calcium carbonate solutions, which can be rationalised based on the release of hydration water upon binding. This mechanism explains how ion clustering can proceed beyond simple ion pairs, yielding PNCs as envisaged by the multiple-binding speciation model, because the process of association is driven by the continuing release of hydration water, not primarily by the formation of ionic bonds as discussed in detail above. Linear pre-nucleation binding profiles (Figure 1) do not categorically exclude the formation of PNCs, as argued elsewhere,[12] but rather imply that all binding events upon PNC formation are energetically more or less equivalent. If Coulomb interactions were to drive the process of ion association and given the charge neutrality of the ion pair, the ion association yielding stable clusters would essentially stop at the ion pair. Moreover, it would be difficult to rationalise why the binding of an ion pair to another ion pair would be energetically equivalent to the binding between individual calcium and carbonate ions. The structural form of the clusters constituting, on average, a linear chain (DOLLOP)[19] is central to understanding this, as the solvent-mediated and entropy-driven binding of an ion to the end of a chain carrying the appropriate charge should be largely inde-

pendent of the chain length. Mechanistically, this is also the reason why ion association can continue without major barriers towards larger species, with release of further water molecules from the hydration shell. Quantitatively, the energetics (Table 1) are consistent with those reported for the self-association of amphiphiles[35] and indicate that PNC formation is likely a more general phenomenon than previously thought.

Experimental Section

Potentiometric Titration Measurements

Titrations of calcium chloride into sodium (bi)carbonate buffers were performed using a commercially available titration system from Metrohm (Filderstadt, Germany). The setup consists of a titration device (Titrando 809), which operates two dosing units (Dosino 807) and provides two ports for the connection of electrodes. The whole assembly is controlled by customised software (Tiamo, v2.3), which allows for precise dosing of titrant solutions and simultaneously reads out the voltages of the connected electrodes. In order to monitor Ca^{2+} concentrations and pH values, a polymer-based ion-selective electrode (ISE, Metrohm, No. 6.0508.110; specified for $T=0$–$40\,^{\circ}C$) and a glass electrode (Metrohm Unitrode, No. 6.0259.100; $T=0$–$100\,^{\circ}C$) were used. Further, a conductivity module (Metrohm, No. 2.856.0010) was connected to the Titrando and equipped with a conductivity probe (Metrohm, No. 6.0910.120; $T=0$–$70\,^{\circ}C$, cell constant $c=0.9\ cm^{-1}$), so that the net specific conductivity could be recorded during the titrations. Experiments were carried out in double-walled vessels (Metrohm, No. 6.1418.250; total volume: 150 mL), through which thermostated oil was circulated utilizing a Julabo (Seelbach, Germany) FP50-ME unit that was regulated by an external Pt100 sensor (Julabo No. 8981003).

For measurements, carbonate buffer (100 mL) was filled into the titration vessel and brought to the desired temperature. Suitable buffers were prepared by mixing solutions (10 mM) of sodium carbonate (Sigma–Aldrich, anhydrous, $\geq$99.95%) and sodium bicarbonate (Riedel-de Haën, $\geq$99.7%) in volume ratios that gave a pH of 9.50 (and a total carbonate concentration of 10 mM). The pH of the buffer was always adjusted at ambient conditions, whereas any temperature-dependent changes occurring were corrected for by adding small aliquots of either NaOH or HCl (both 1 M, obtained from Merck, p.a.) after the targeted temperature had been reached. After immersion of all needed probes and sufficient periods of equilibration, the titration routine was initiated and $CaCl_2$ (10 mM, obtained by dilution of a 0.1 M ion standard solution from Metrohm, No. 6.2301.070) was added at a constant rate of $0.01\ mL\,min^{-1}$. The pH of the buffer was kept constant at 9.50 by automatic counter-titration of NaOH (10 mM, Alfa Aesar, standard solution) while, simultaneously, all dosed volumes as well as the actual pH, specific conductivity and calcium potential were continuously recorded. During the measurements, the vessels were firmly closed by a cap, so as to avoid distinct outgassing of CO_2 from the buffer and evaporation of water. At each investigated temperature, at least three (normally 4–5) independent experiments were performed to ensure reproducibility. After each experiment, the titration vessel was emptied and filled with acetic acid (10%), so as to remove any precipitated carbonate material from the glass walls, the immersed electrodes and the burette tips. After two such cycles of acid treatment, all equipment was rinsed thoroughly with Milli-Q water and dried with dust-free tissue paper.

All sensors were calibrated at the respective target temperature prior to measurement. In case of the Ca^{2+}-selective electrode, this was achieved by titrating $CaCl_2$ (10 mM) into water that had previously been adjusted to pH 9.50 by addition of NaOH (10 mM). For calibration, the same routine was used as in the actual measurements (just replacing carbonate buffer by water, where no Ca^{2+} binding is expected). However, to avoid significant uptake of CO_2 from the atmosphere, a gentle stream of nitrogen was flushed through the sample chamber in calibrations at lower temperatures. However, this was no longer necessary starting from about $40\,^{\circ}C$, where the internal pressure in the vessel intrinsically prevented any significant inward diffusion of gases. The pH electrode was calibrated with buffers obtained from Metrohm (nominal pH values at $25\,^{\circ}C$: 4.00, 7.00 and 9.00), taking into account temperature-induced changes in the actual pH of the buffers. Finally, the cell constant of the conductivity probe was determined regularly by measuring the absolute conductivity of a potassium chloride standard solution (Merck, CertiPUR Standard, 1.41 mS cm), which thus allowed specific conductivities κ to be derived from the experimental data.

Please see the SI for details on data evaluation (section 1.1).

Isothermal Titration Calorimetry

ITC analyses of ion association in pre-nucleation $CaCO_3$ solutions were performed using microcalorimeters from MicroCal (Model iTC200) and TA Instruments (Model Nano ITC). The ITC devices consist of two cells, sample and reference, both having total volumes of 205 (iTC200) or 950 μL (Nano ITC). The sample cell was filled with carbonate buffer (4 mM, set to pH 9.50), into which calcium chloride solution (4 mM, brought to pH 9.50 by 0.1 M NaOH) was added in given volume increments through a syringe, while the supplied software recorded the excess heating rate. The particular volumes of the injections and intervals between each injection were tuned with respect to thermal equilibration of the cells. The final optimised protocols were as follows: a) iTC200: 0.2 μL for the initial injection, 0.5 μL for the subsequent 12 steps, and 1.0 μL for all remaining injections; b) Nano ITC: 5.14 μL for all 40 titration steps. The interval between injections was 300 s in both setups. The presence of gas bubbles in the cells was minimised by degassing the solutions in vacuum prior to usage and careful filling of the cells. Measurements at $25\,^{\circ}C$ were performed at least in triplicate on each of the calorimeters, both in ambient and Ar atmospheres, with no noticeable difference in the resulting data and good reproducibility. Titrations at $40\,^{\circ}C$ were only conducted on the Nano ITC instrument, again in three independent repetitions. For the reference experiments, meant to determine the heats of dilution, water and $CaCl_2$ solutions were adjusted to pH 9.50 by addition of NaOH (0.1 M). Between measurements, the cells and syringe were cleaned by several successive Milli-Q water washing steps, which was sufficient for the investigated conditions as no solid mineral phase precipitated in the experiments.

Please see the Supporting Information for details on data evaluation (section 1.2).

Molecular Dynamics (MD) Simulations

All simulations were carried out using molecular dynamics based on a previously derived force field.[19,48] Simulations were performed for a model system containing two ions in a cubic cell with 2448 water molecules. Initial equilibration was performed in the *NPT* ensemble using a Nosé-Hoover thermostat and barostat, with

a time step of 1 fs. After constant pressure equilibration of the cell under isotropic constraints at the temperature of interest, the free energy was evaluated in the *NVT* ensemble using the multiple walkers metadynamics technique.[31] Two collective variables were used simultaneously, namely the Ca–C distance (to capture the separation of ions) and the coordination number of calcium by water (to ensure that the kinetics of water exchange do not impact on the results). In the calculation of the calcium–water coordination number, a switching function was employed that decays to zero within the second peak in the Ca–O radial distribution function. In order to ensure the convergence of the free energy calculations, a well-tempered algorithm[49] was employed with a bias factor of 5. A total of 25 walkers[50] for each simulation was used, with each walker executing between 6 and 10 ns. All simulations were performed using the program LAMMPS[51] with the PLUMED[52] plug-in for metadynamics (release 2.0), and some in house modifications for the implementation of the force field. All the details of the computational procedure can be found in ref. [48]. The ion pairing calculation at each temperature has been repeated three times starting from independent starting configurations to improve the statistics. The enthalpic and entropic terms have been obtained from a linear fit to the ion pairing free energies calculated at different temperatures and the uncertainties reported in Table 1 are those obtained from the fitting method.

Acknowledgements

The authors thank H. P. Kaub and S. Deck (BASF SE) for help with some of the ITC measurements. D.G. is supported by the Zukunftskolleg of the University of Konstanz and the Fonds der Chemischen Industrie. D.G. and J.K.B. acknowledge generous support of the Young Scholar Fund of the University of Konstanz. P.R. and J.D.G. acknowledge funding from the Australian Research Council (FT130100463, DP160100677) and the use of resources provided by the Pawsey Supercomputing Centre and the National Computational Infrastructure with funding from the Australian Government and the Government of Western Australia.

Keywords: calcium carbonate · entropy · ion association · ion pairing · pre-nucleation clusters

[1] *Handbook of Industrial Crystallization* (Ed.: A. S. Myerson), Butterworth-Heinemann, Boston, **2002**.
[2] J. Rieger, M. Kellermeier, L. Nicoleau, *Angew. Chem. Int. Ed.* **2014**, *53*, 12380 – 12396; *Angew. Chem.* **2014**, *126*, 12586 – 12603.
[3] M. Volmer, A. Weber, *Z. Phys. Chem.* **1925**, *119*, 277 – 301.
[4] R. Becker, W. Döring, *Ann. Phys.* **1935**, *24*, 719 – 752.
[5] R. J. Davey, S. L. M. Schroeder, J. H. ter Horst, *Angew. Chem. Int. Ed.* **2013**, *52*, 2166 – 2179; *Angew. Chem.* **2013**, *125*, 2220 – 2234.
[6] D. Gebauer, H. Cölfen, *Nano Today* **2011**, *6*, 564 – 584.
[7] D. Erdemir, A. Y. Lee, A. S. Myerson, *Acc. Chem. Res.* **2009**, *42*, 621 – 629.
[8] R. P. Sear, *Int. Mater. Rev.* **2012**, *57*, 328 – 356.
[9] Q. Hu, M. H. Nielsen, C. L. Freeman, L. M. Hamm, J. Tao, J. R. I. Lee, T. Y. J. Han, U. Becker, J. H. Harding, P. M. Dove, et al., *Faraday Discuss.* **2012**, *159*, 509 – 523.
[10] D. Gebauer, M. Kellermeier, J. D. Gale, L. Bergström, H. Cölfen, *Chem. Soc. Rev.* **2014**, *43*, 2348 – 2371.
[11] J. Baumgartner, A. Dey, P. H. H. Bomans, C. Le Coadou, P. Fratzl, N. A. J. M. Sommerdijk, D. Faivre, *Nat. Mater.* **2013**, *12*, 310 – 314.
[12] W. J. E. M. Habraken, J. Tao, L. J. Brylka, H. Friedrich, L. Bertinetti, A. S. Schenk, A. Verch, V. Dmitrovic, P. H. H. Bomans, P. M. Frederik, et al., *Nat. Commun.* **2013**, *4*, 1507.
[13] P. R. ten Wolde, D. Frenkel, *Science* **1997**, *277*, 1975 – 1978.
[14] O. Galkin, P. G. Vekilov, *Proc. Natl. Acad. Sci. USA* **2000**, *97*, 6277 – 6281.
[15] P. G. Vekilov, *Cryst. Growth Des.* **2010**, *10*, 5007 – 5019.
[16] H. Lowenstam, S. Weiner, *On Biomineralization*, Oxford University Press, New York, **1989**.
[17] J. Geyssant, E. Huwald, D. Strauch, *Calcium Carbonate: From the Cretaceous Period into the 21st Century*, Birkhäuser, Basel, Boston, **2001**.
[18] M. H. Nielsen, S. Aloni, J. J. De Yoreo, *Science* **2014**, *345*, 1158 – 1162.
[19] R. Demichelis, P. Raiteri, J. D. Gale, D. Quigley, D. Gebauer, *Nat. Commun.* **2011**, *2*, 590.
[20] L. Sapir, D. Harries, *Curr. Opin. Colloid Interface Sci.* **2016**, *22*, 80 – 87.
[21] L. Sapir, D. Harries, *Curr. Opin. Colloid Interface Sci.* **2015**, *20*, 3 – 10.
[22] D. Gebauer, A. Völkel, H. Cölfen, *Science* **2008**, *322*, 1819 – 1822.
[23] M. Kellermeier, H. Cölfen, D. Gebauer, in *Methods in Enzymology*, Academic Press, Burlington, **2013**, pp. 45 – 69.
[24] M. Kellermeier, A. Picker, A. Kempter, H. Cölfen, D. Gebauer, *Adv. Mater.* **2014**, *26*, 752 – 757.
[25] E. M. Pouget, P. H. H. Bomans, J. A. C. M. Goos, P. M. Frederik, G. de With, N. A. J. M. Sommerdijk, *Science* **2009**, *323*, 1455 – 1458.
[26] M. Kellermeier, D. Gebauer, E. Melero-García, M. Drechsler, Y. Talmon, L. Kienle, H. Cölfen, J. M. García-Ruiz, W. Kunz, *Adv. Funct. Mater.* **2012**, *22*, 4301 – 4311.
[27] L. Plummer, E. Busenberg, *Geochim. Cosmochim. Acta* **1982**, *46*, 1011 – 1040.
[28] P. Raiteri, J. D. Gale, D. Quigley, P. M. Rodger, *J. Phys. Chem. C* **2010**, *114*, 5997 – 6010.
[29] R. M. Fuoss, C. A. Kraus, *J. Am. Chem. Soc.* **1933**, *55*, 1019 – 1028.
[30] M. A. Bewernitz, D. Gebauer, J. R. Long, H. Cölfen, L. B. Gower, *Faraday Discuss.* **2012**, *159*, 291 – 312.
[31] A. Laio, M. Parrinello, *Proc. Natl. Acad. Sci. USA* **2002**, *99*, 12562 – 12566.
[32] M. Kinoshita, *Int. J. Mol. Sci.* **2009**, *10*, 1064 – 1080.
[33] P. L. Privalov, G. I. Makhatadze, *J. Mol. Biol.* **1993**, *232*, 660 – 679.
[34] M. Colombo, D. Rau, V. Parsegian, *Science* **1992**, *256*, 655 – 659.
[35] S. Paula, W. Süs, J. Tuchtenhagen, A. Blume, *J. Phys. Chem.* **1995**, *99*, 11742 – 11751.
[36] P. W. Snyder, J. Mecinovic, D. T. Moustakas, S. W. Thomas, M. Harder, E. T. Mack, M. R. Lockett, A. Heroux, W. Sherman, G. M. Whitesides, *Proc. Natl. Acad. Sci. USA* **2011**, *108*, 17889 – 17894.
[37] P. Prapaipong, E. L. Shock, C. M. Koretsky, *Geochim. Cosmochim. Acta* **1999**, *63*, 2547 – 2577.
[38] P. F. Damasceno, M. Engel, S. C. Glotzer, *ACS Nano* **2012**, *6*, 609 – 614.
[39] P. G. Vekilov, A. R. Feeling-Taylor, D. N. Petsev, O. Galkin, R. L. Nagel, R. E. Hirsch, *Biophys. J.* **2002**, *83*, 1147 – 1156.
[40] F. Jalilehvand, D. Spångberg, P. Lindqvist-Reis, K. Hermansson, I. Persson, M. Sandström, *J. Am. Chem. Soc.* **2001**, *123*, 431 – 441.
[41] J. L. Fulton, S. M. Heald, Y. S. Badyal, J. M. Simonson, *J. Phys. Chem. A* **2003**, *107*, 4688 – 4696.
[42] W. A. Adeagbo, N. L. Doltsinis, M. Burchard, W. V. Maresch, T. Fockenberg, *J. Chem. Phys.* **2012**, *137*, 124502.
[43] Y. Kameda, M. Sasaki, S. Hino, Y. Amo, T. Usuki, *Physica B* **2006**, *385 – 386*, 279 – 281.
[44] F. Bruneval, D. Donadio, M. Parrinello, *J. Phys. Chem. B* **2007**, *111*, 12219 – 12227.
[45] J. D. Dunitz, *Science* **1994**, *264*, 670 – 670.
[46] P. Raiteri, J. D. Gale, *J. Am. Chem. Soc.* **2010**, *132*, 17623 – 17634.
[47] E. Königsberger, L.-C. Königsberger, H. Gamsjäger, *Geochim. Cosmochim. Acta* **1999**, *63*, 3105 – 3119.
[48] P. Raiteri, R. Demichelis, J. D. Gale, *J. Phys. Chem. C* **2015**, *119*, 24447 – 24458.
[49] A. Barducci, G. Bussi, M. Parrinello, *Phys. Rev. Lett.* **2008**, *100*, 020603.
[50] P. Raiteri, A. Laio, F. L. Gervasio, C. Micheletti, M. Parrinello, *J. Phys. Chem. B* **2006**, *110*, 3533 – 3539.
[51] S. Plimpton, *J. Comput. Phys.* **1995**, *117*, 1 – 19.
[52] G. A. Tribello, M. Bonomi, D. Branduardi, C. Camilloni, G. Bussi, *Comput. Phys. Commun.* **2014**, *185*, 604 – 613.

Manuscript received: June 17, 2016
Accepted Article published: August 19, 2016
Final Article published: September 14, 2016